EFDA–JET–PR(12)13

R. Albanese, F. Maviglia, P.J. Lomas, A. Manzanares, M. Mattei, A. Neto,
F.G. Rimini, P.C. de Vries and JET EFDA contributors

Experimental Results with an Optimised Magnetic Field Configuration for JET Breakdown

Experimental Results with an Optimised Magnetic Field Configuration for JET Breakdown

R. Albanese[1], F. Maviglia[1], P.J. Lomas[2], A. Manzanares[3], M. Mattei[4], A. Neto[5], F.G. Rimini[2], P.C. de Vries[6] and JET EFDA contributors*

JET-EFDA, Culham Science Centre, OX14 3DB, Abingdon, UK

[1]Associazione EURATOM-ENEA-CREATE, University di Napoli Federico II, Via Claudio 21, 80125, Napoli, Italy.
[2]EURATOM-CCFE Fusion Association, Culham Science Centre, OX14 3DB, Abingdon, OXON, UK
[3]Asociaciòn EURATOM-CIEMAT para Fusiòn, CIEMAT, Madrid, Spain.
[4]Associazione Euratom-ENEA-CREATE, DIAM, Seconda Università degli Studi di Napoli, Via Roma 29, 80131 Aversa (CE), Italy.
[5]Associação Euratom-IST, Instituto de Plasmas e Fusão Nuclear, Av. Rovisco Pais, 1049-001 Lisboa, Portugal.
[6]FOM Institute DIFFER, Association EURATOM-FOM, Nieuwegein, The Netherlands.
** See annex of F. Romanelli et al, "Overview of JET Results", (23rd IAEA Fusion Energy Conference, Daejon, Republic of Korea (2010)).*

Preprint of Paper to be submitted for publication in
Nuclear Fusion

ABSTRACT.
Experiments and modelling have been carried out in order to optimize the magnetic field null during breakdown at JET. Such optimization may prove to be essential to reliable plasma initiation at low voltage, e.g. in ITER where the value of the electric field available will be limited to 0.33 *V/m*.

A 2 dimensional FEM electromagnetic model has been employed to predict the stray field configuration during JET breakdown. This model includes the active Poloidal Field (PF) circuits, a description of the passive structure and the JET magnetic circuit. In particular the model includes the gap in the top of the iron circuit (but not at the bottom) which introduces a perturbing field, with radial and vertical components, not previously considered. A number of experiments were run by using the optimised magnetic null configuration, allowing to achieve a more robust breakdown at low electric field. The model predictions were validated by using the recordings from the fast visible camera. The optimised position and dynamics of the plasma start lead to a smoother behaviour of the JET radial field control system, far from the amplifiers limits. Finally, an important indication was obtained on the precision needed for the active currents measurements during the low electric field breakdown relevant in perspective of the ITER real-time acquisition system.

1. INTRODUCTION

The plasma formation is achieved in a tokamak fusion device by ionising a gas present in a toroidal vacuum chamber, with the application of a toroidal electric field. One important parameter for the breakdown success is the initial electric field E_0. The typical electric field of present tokamaks is about 1 *V/m*, while in the current ITER design it is limited to a value of about 0.33 *V/m* [1], leaving a lower margin for the breakdown success. Other important breakdown parameters are the poloidal and toroidal magnetic field configuration, the magnetic null position and extent of the low field region. These determine the connection length $L_c(1)$ along field lines to the vessel [2], defined as:

$$L_c = \frac{1}{4}\frac{a_{null} B_\phi}{< B_z >} ; \qquad (1)$$

where a_{null} is the size of the field minimum, B_ϕ is the toroidal field, and $<B_z>$ is the average stray field over the null. In order to have a successful avalanche phase it is necessary to maximize L_c by minimization of $<B_z>$ and maximization of a_{null}. At JET the low electric field breakdowns have a higher occurrence of Non Sustained Breakdown (NSB), which preclude the execution of some experiments and reduce precious experimental time. At JET, it is difficult to use magnetic measurements to control the evolution of the nascent plasma because of noise, accuracy, bit size and offsets. ITER will have in addition further complications such as ferromagnetic inserts and vessel eddy currents which will have larger effects than in JET, as well as the fact that different amplifiers will be used to produce the primary transformer action, with a consequently high synchronization precision required. For these reasons in ITER a larger connection length will be required to match the reduced electric field. This paper presents the optimization of the magnetic field configuration

for JET breakdown. This exploited an accurate electromagnetic JET model provided by the 2D axisymmetric finite element code CREATE-L [3]. In the first section of this paper the modelling of the stray field in the JET machine is presented. The second part is devoted to the static electromagnetic analysis of JET breakdown conditions. The experimental results of the breakdown optimization will be presented in the last part of the paper comparing the model prediction with the experimental measurements and the recordings of the new JET fast visible camera [4].

2. MODEL OF THE JET POLOIDAL FIELD SYSTEM AND MAGNETIC CIRCUIT

The electromagnetic model used for the breakdown study includes the Poloidal Field (PF) circuits, the conducting structures with 3-D corrections and an equivalent 2-D axisymmetric model of the iron core [3]. The JET PF system is composed of eight sets of coils. Four of those are up down symmetric and are named from P1 up to P4 while the remaining four are placed in the lower part of the in-vessel, named divertor region, called D1 to D4. Ten different amplifiers supply circuits that use different parts of the coils. The circuits used at JET during the breakdown phase, represented in Fig. 1, are the primary, P1 (including the coils P1C, P1U, P1L, P3MU and P3ML), vertical, P4 (including the coils P4U and P4L), and radial PF circuits (including the coils P2RU, P3RU, P2RL and P3RL). The first is the primary of an electric transformer which drives the plasma current. According to the different possible configurations used, it can provide initial P1 current values in the range [7, 40] *kA*, with the JET iron fully saturated, or P1 current close to zero, with residual magnetization present in the magnetic circuit. The vertical field circuit can be used in open loop current control or combined with plasma flux control. The radial field circuit combines compensation of the radial field due to the passive currents flowing in the conducting supporting structures of the divertor coils with plasma velocity feedback.

The passive conducting structures, which are described in detail in [5], included in the model are: Vacuum Vessel (VV), Restraint Rings (RR), Mechanical Structure (MS) and the divertor Mark 2 supporting structure (MK2), mentioned above. The MK2 structure is the only up-down asymmetric passive structure and plays a fundamental role on the magnetic field null position during the breakdown phase. For the purpose of this paper no dynamic simulation will be included, considering the effect of the eddy currents adequately compensated by the system, leaving a more detailed treatment to a separate work [6].

Finally, the model of the JET iron includes the presence of a 3 *mm* gap in the magnetic circuit, located in the upper part of the machine at the vertical position $z = 4.45\ m$, but there is no corresponding gap at z=-4.45 *m* [7]. The inclusion of this detail, never previously considered, is significant at the level of stray field for avalanche conditions as described in the next section.

3. MODELLING OF JET MAGNETIC CONFIGURATION

Presently at JET the experimental magnetic measurements do not take into account the residual magnetization of the iron. The time integrators of the pickup coils are in fact reset to zero at the

beginning of the pulse, when only leakage currents are present, and neglects the iron residual magnetization B_0, which is of the order of a fraction of *mT* in the vacuum chamber region. This uncertainty, together with the inaccurate toroidal pickup magnetic field compensation, do not permit the use of integrated magnetic measurements during the breakdown, due to the required precision of the stray field control below the fraction of *mT* for a successful discharge [2].

The modelling analysis has been performed for a wide range of different initial values of primary circuit and vertical field, influencing the stray field configuration. The effect of the presence of the air-gap in the magnetic circuit has been assessed for a series of breakdown configurations. A typical value of the field due to the gap is about 0.5 *mT* in the centre of the chamber, with radial and vertical components. This perturbing field is of the same order of magnitude of the typical value that was previously considered for $< B_z >$ used in equation (1) [2]. The ideal hexapolar null, under the influence of the field due to the gap, splits in the direction of the perturbing field into two quadrupolar nulls, located in the inboard-lower and upper-outer region of the vacuum chamber, as shown in Fig. 2. In this condition the inboard-lower null is expected to be preferred for plasma formation due to the higher electric field, the connection length being similar for the two cases. As observed in Ref. [7] the avalanche evolves dynamically towards a region that leans on the part of the first wall where the angle between the force on the plasma and the normal unit vector is larger than 90 degrees. In the poloidal plane such a region is delimited by the points where the stray field is perpendicular to the first wall. The plasma is then pushed down in the divertor region and finally, for a successful breakdown, is pulled up toward the outer wall by the Vertical Stabilization system (VS), which acts on the radial field circuit, with a large ERFA current excursion. However, in a certain number of JET experiments, especially in the more fragile low voltage breakdown, the radial field circuit action is not sufficient, with the plasma terminating in the divertor region.

4. OPTIMIZATION OF THE BREAKDOWN MAGNETIC CONFIGURATION

The aim of the magnetic null optimization was to avoid the downward movement of the plasma, in the divertor region, during the early dynamic phase, to reduce the NSB occurrences and reduce the control action of the VS system. The application of a corrective radial field would rotate the position of the two quadrupolar nulls anticlockwise. This is done, as shown in Fig. 3, by adding a constant "radial bias" current in the ERFA circuit, carried out in order to assess the calculated correction field. With positive radial bias the upper-inner field null is expected to be preferred for the plasma formation, having higher electric field whilst the connection length remains comparable in the two null regions.

4.1. EXPERIMENTAL RESULTS FROM BREAKDOWN OPTIMIZATION ON VS SYSTEM

A number of experiments have been performed with the standard breakdown recipes, with zero radial bias and with added radial bias. The JET VS system [8], which drives the ERFA circuit, allows a radial field current waveform to be added to the value of the estimated current in passive structure

to be compensated, useful in the dynamic phase [7]. The experimental data shown in Fig. 4 are the currents in the three active PF circuits, named IP1 (primary), IP4 (vertical field) and IERFA (radial field) for a shot-to-shot scan of bias radial field. Another interesting experimental signal was the vertical velocity loop control request, named VFB, which is used by the VS system to control to zero the plasma vertical speed. The latter control loop switches from "no-plasma" to "plasma" status when the plasma current value, IPLA, exceeds a preset value, normally set to 47 *kA*. Both the contributions of the radial field current loop and velocity loop give the indication of the "effort" required by the VS system to correct the dynamic evolution respectively of early plasma position and velocity. A number of pulses have been run using a predicted range of values of the correction radial field bias and the standard (no bias) case. The radial bias scan has been run with the same primary pre-programmed currents and same initial IP4 waveforms. As predicted from the model reconstruction, the plasma started in the inner wall further from the divertor region with higher radial bias, as observed in the first available visible frames from the slow visible camera in Fig. 5. The experiments confirmed the optimal radial bias value, predicted by the model, to be given to have the ionization cloud centred on the coordinate $z = 0$. As expected the effect of the optimised starting position brought as a consequence a smoother behaviour of the VS system, with a lower excursion of the ERFA current, proportional to the vertical position correction needed, far from the amplifier limits, normally equal to ±5 *kA*.

An improved control behaviour was achieved also on the velocity control loop, with a reduced voltage request sent to the radial field amplifier for the optimised plasma starting point cases. The Fig. 4 shows that while for all the radial bias corrected cases the velocity control action, the resulting voltage request (VFB), oscillates within the range of 10^4 *V*, for the standard case it presents a very large peak, always in the same direction, of the order of 10^5-10^6 *V*. It is important to notice that the peak in the velocity loop control is proportional to the estimation of the plasma vertical speed and is present at the time when the plasma is pulled out from the divertor region, as confirmed from the fast visible camera images discussed in paragraph 4.3, and occurs only for the pulses without bias. Statistical analyses have been performed for all the plasma experiments run at JET after the installation of the new beryllium wall, for all the different breakdown recipes characterized by initial primary current that span in the range [7, 40] *kA*. A figure of merit, related to the maximum absolute variation of IERFA (radial field current), is defined in the following time range of interest:

$$f.o.m = \min\left(\left|\Delta IERFA\right|\right), \text{ with } t \in \lfloor t_{|IPLA|>47\kappa A};\ 0.06s \rfloor; \tag{2}$$

where $t_{|IPLA|>47\kappa A}$ represents the time instant when $|IPLA| > 47\kappa A$, which assumes different values, depending of the pre-programmed plasma current ramp-up slope, and 0.06 *s* it is a chosen arbitrary time when in all the successful breakdowns the plasma column is positioned on the outer limiter. Fig. 6 is shows the initial value of the ERFA current on the abscissa, proportional to the requested correction radial field, while in the ordinate axis is reported the *f.o.m* considered in (2). By using the

optimised radial bias correction, the maximum absolute variation of the ERFA current is reduced by a factor of about 4÷5, allowing a larger clearance from the amplifier limits. The standard breakdown recipe is more fragile and results in a larger occurrence of NSB. This is more important for the low electric field breakdown, where the plasma ionization success margin is already reduced.
Since its introduction, the radial bias correction as described in this article, has been widely used and is currently applied in the vast majority of the experiments.

4.2. STUDY OF THE INFLUENCE OF THE MEASUREMENT OFFSET INTRODUCED BY THE NEW VS SYSTEM

One feature that had gone unnoticed since the installation of a new vertical stabilization system VS in 2009 [8] was revealed by these studies and that was varying offsets introduced inadvertently by the data acquisition system. These spurious offsets stepped from value to value over weeks, for example a typical offset in the range of ±50 *A* was present in the ERFA current measurement, equivalent approximately to ±0.2 *mT* in the centre of the chamber. Large offsets corresponded to periods where low voltage breakdown was unreliable or even failed totally. Normal high voltage breakdown was unaffected. A 0.2 *mT* offset is small in terms of connection length and so stimulated further experimental studies at low electric field, i.e. $E_0 < 0.3$ *V/m* described in section 4.3. The precision required for the measurements in low electric field breakdown conditions may represents an important information for the design of the acquisition system of machines with a limited E_0 value, i.e. ITER. 4.3. Images from the fast visible camera during the breakdown optimization experiments
The fast visible camera of JET [4] has been improved with the installation of a two-step image intensifier. This new setup enables smaller exposure times at a high number of frames per second, which increases the possibility to study the low light conditions of the preliminary plasma formation phase with higher temporal resolution. This new setup has two configurations for studies of plasma breakdown. The first configuration keeps the same spatial resolution as previous studies (~1 *cm/px*), with an image size of the detector of 272x384 *pixels* for the whole half-torus, and doubles the frame speed to 1000 frame/sec. The second configuration increases the temporal resolution with a frame speed of 7500 *frames/sec*, while the spatial resolution is decreased to 20x14 *cm/px* with an image size of the detector of 176x256 *pixels* for the whole half-torus. Neither configuration uses filters to record the image. The new enhanced fast visible camera has been used with success during several sessions of breakdown optimization experiments to validate the model predictions and the experimental measurements.

A first series of experiment was run with initial primary current in the range [7, 40] *kA*, with JET iron fully saturated in the central column. Fig. 7 shows the comparison of a standard case with the optimised case. As suggested by the model predictions and by the VS measurements, it was confirmed that for all the cases which include the radial bias the first visible images of the ionization cloud appear centred in the inner wall, farther from the divertor region for higher correction bias, with generally more extended and clearer breakdown area, comparing with the standard case. It is

shown in the subsequent captured images that the optimised pulses present a lower light emission from the divertor region and move to the outer wall earlier comparing to the standard case.

For the standard not optimised case, it was instead confirmed, by superposing the camera images to the current experimental measurements, that the plasma start in the lower inner wall and then is pushed downward, with an higher visible light emission from the divertor due to the recycling gas. The plasma remains in the lower part of the vessel until the vertical velocity loop is switched to "plasma" status. At this point the plasma is pulled up by a more aggressive control action of the VS system which leads to a large variation of the ERFA current, comparing with the optimised case. It is possible to notice in the camera recording that if the vertical velocity control loop action becomes too aggressive, once the plasma is pulled up from the divertor region, it is driven towards the upper part of the chamber, coming in contact with more fragile parts of the machine. It was also recorded a number of pulses where the plasma gets trapped in the divertor region and there it disappears. This happens if the radial field action is not sufficient to correct the initial non optimised plasma position, leading to a non sustained plasma breakdown. The result obtained for the standard not optimised configuration is coherent with the observation obtained in the past using the fast visible camera with the carbon wall [7], where for all the available recordings it was shown that the plasma was always pushed in the divertor region during the breakdown and then pulled up by the VS system, for the successful attempts.

The optimised radial bias recipe was extended to a second set of experiments with initial primary current close to 0 during the breakdown. In this condition the JET iron is partially magnetized by a leakage current present in the same primary circuit of the order of hundred amperes, of the same negative sign considered in the previous case. The model magnetic null calculation precision is less accurate in this case because the uncertainties (e.g. offsets) are larger relative to the measured value. Another perturbing effect is due to the evolution of the active PF currents and the induced vessel and in-vessel eddy currents, which delay the entrance of the magnetic null in the chamber once the vertical field is driven to zero after having an off-set to suppress plasma formation before the loop voltage is high enough. A full bias scan has been implemented for a series of pulses with ITER like initial electric field $E_0 = 0.3\ V/m$, in order to optimize the null position and to take into account the radial field current offset introduced by the VS system, starting from negative up to positive discrete values, including the standard non bias case (Fig. 8). By applying an optimised radial bias of $+100\ A$, the first available image shown a more centred and extended breakdown area, while in the standard and negative sign bias ($-50\ A$) the ionization cloud appears in the upper part of the machine. In the subsequent time instant is shown how both the configuration with positive bias ($+50\ A$ and $+100\ A$) are successfully lying in the outer wall, while the negative and zero bias are in the divertor region, respectively deep and less deep as expected. In the final sequence of images the positive bias pulses are still in the outer wall, as desired, with a smoother radial field excursion at higher bias. The negative bias pulse instead fails disappearing deeper in the divertor region, without even triggering the vertical velocity loop plasma "ON" status. In the standard configuration

the plasma is eventually pulled out from the divertor region with amore aggressive action of the vertical velocity loop, comparing with the optimised case. The optimised configuration together with the compensation of the measurements offset, permitted to achieve a more robust breakdown and allowed to re-establish at JET a more reliable low electric field "ITER like" breakdown down to $E_0 = 0.25\ V/m$, with the new beryllium wall and VS system.

CONCLUSIONS

This paper presents the experimental results of the optimization of the magnetic configuration during the breakdown phase at JET. The breakdown may have a major impact on the experimental activity of a tokamak, and can affect availability for the scientific activity. For this reason it is important reduce the NSB occurrences by optimizing the relevant parameters. This may prove to be particularly important for future experimental machines where the value of the electric field available will be limited, like ITER where E_0 will be limited to 0.33 V/m, against the value of about 1 V/m of the present tokamaks, leaving a lower margin of error and potentially a higher breakdown failure rate. In ITER there will be further perturbing effects which may affect the precision of stray field control during the breakdown phase such as the ferromagnetic inserts, the integrated measurement errors, the eddy currents and the high synchronization precision required for the different amplifiers that will be used to produce the primary transformer action.

A finely tuned 2D FEM electromagnetic model, with a precision of the order of a fraction of mT has been employed to predict the stray field configuration during JET breakdown and verified by the effect on the plasma starting position against the fast camera images. This model includes the active PF circuits, a description of the passive structure and the JET magnetic circuit. The presence of the air-gap in the iron model, present at JET at the ordinate z = +4.5 m, and not at z = -4.5 m induce a perturbing field, with radial and vertical components, in the centre of the camber of the order of 0.5 mT during breakdown phase. The ideal hexapole magnetic null, which would be present in an up-down symmetric case, splits in two quadrupolar nulls in the direction of the perturbing field. In this condition the inboard lower null is expected to be preferred for plasma formation due to the higher electric field. In the breakdown phase of all past JET pulses the plasma was then pushed down in the divertor region by the radial field produced by the passive current flowing in the divertor conduction structures MK2. Finally, for a successful breakdown the plasma was then pulled out by the VS system, or terminated in the divertor region if the radial field circuit action was not sufficient.

An optimization was performed in order to correct the perturbing field by scanning the radial field current bias over a range suggested by the calculation. The new optimised plasma initial position avoids the plasma moving to the divertor region, and makes the breakdown more robust, with a lower occurrence of failed attempts. The new enhanced fast visible camera has been used to validate the model prediction on plasma start-up and dynamic evolution. The optimised initial magnetic null position leads to an improved behaviour of the VS system, with a smaller radial

field current excursion of a factor 4÷5, far from the amplifier limits. Thanks to the re-optimised breakdown recipe it has been possible to re-establish at JET a reliable low electric field "ITER like" breakdown down to $E_0 = 0.25\ V/m$ with the new beryllium wall and VS system. The low electric field breakdown success it is at JET particularly sensitive to any error field, being not possible to successfully start the plasma for $E_0 < 0.3\ V/m$ with radial field errors of the order $\pm 0.5\ mT$. It was proved essential to take into account and correct the offset that can be generated by the new vertical stabilization system particularly on the radial field current measurement, to a precision better than $\pm 50\ A$, corresponding to a stray field of $\pm 0.2\ mT$, for the "ITER like" low electric field breakdowns.

ACKNOWLEDGMENTS

This work was supported by EURATOM and carried out within the framework of the European Fusion Development Agreement. The views and opinions expressed herein do not necessarily reflect those of the European Commission. The authors wish to thank A.C.C. Sips for his valuable comments and suggestions.

REFERENCES

[1]. A.C.C. Sips, et al., Nuclear Fusion **49** (2009) 085015 (11pp).

[2]. B. LLoyd, et al., Nuclear Fusion **31** (1991) 2031.

[3]. R. Albanese, et al., Nuclear Fusion, **38**, 1998, pp. 723–738.

[4]. J.A. Alonso, et al., Proc. 34th EPS Conference on Plasma Physics, Warsaw, Poland, ECA Vol.31F, P-2.124 (2007). Web link: http://epsppd.epfl.ch/Warsaw/pdf/P2_124.pdf.

[5]. R.Albanese, et al., Fusion Engineering and Design **66-68** (2003) pp. 715-718.

[6]. F. Maviglia, et al., 7th Workshop on Fusion Data Processing Validation and Analysis. Frascati 26-28 March 2012" Web link: http://www.fusione.enea.it/EVENTS/eventifiles validation7-2012/workshop-slides/2ndday/FMaviglia%20-%20Frascati%20WS%202012pdf.

[7]. F. Maviglia, et al., Fusion Engineering and Design **86** (2011) pp. 675–679.

[8]. F. Sartori, et al., Fusion Engineering and Design **83** (2008) pp. 202–206.

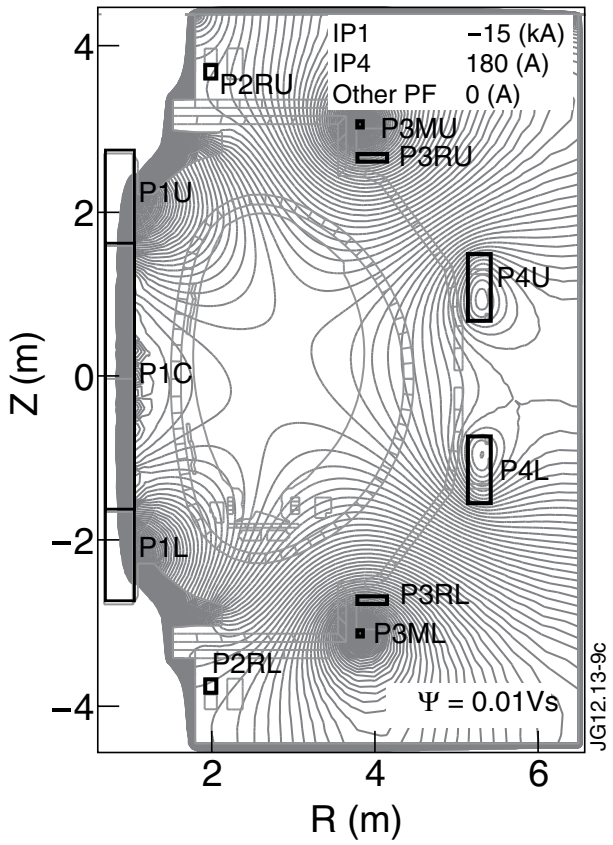

Figure 1: Model of the poloidal field circuits used at JET during the breakdown phase and example of the relative flux map static reconstruction. In the picture are represented the primary (including the coils P1C, P1U, P1L, P3MU and P3ML), the vertical (including the coils P4U and P4L), and the radial circuit (including the coils P2RU, P3RU, P2RL and P3RL).

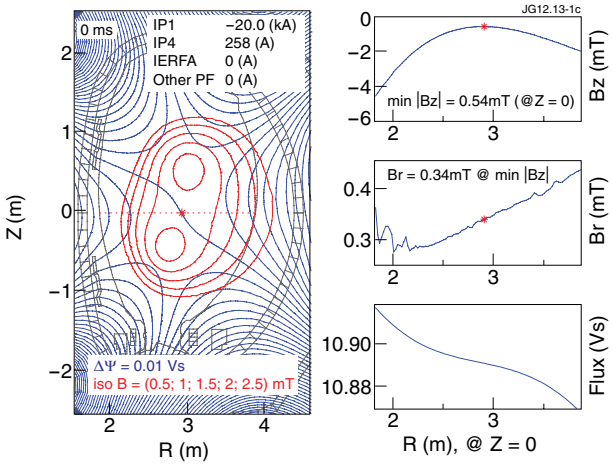

Figure 2: Static equilibrium model reconstruction of magnetic flux and field for a JET breakdown configuration with prescribed primary (IP1) and vertical (IP4) circuit currents. In the plots on the right the values of Br, Bz and flux at z = 0 are shown.

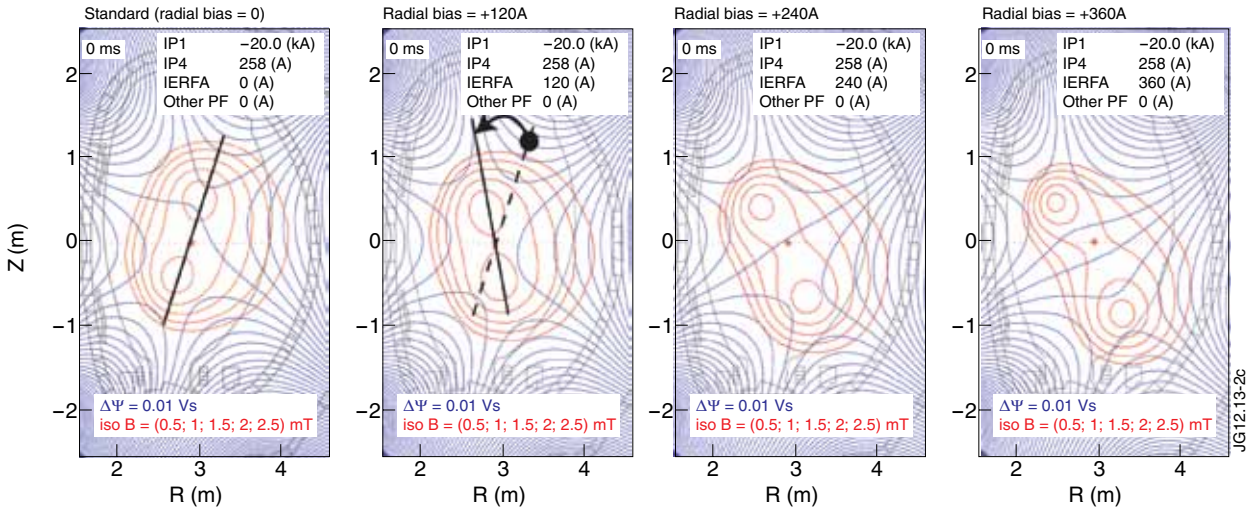

Figure 3: Static equilibrium calculation of magnetic flux and field for a standard breakdown configuration, in the left picture, and a number of radial field correction values, in the following three pictures.

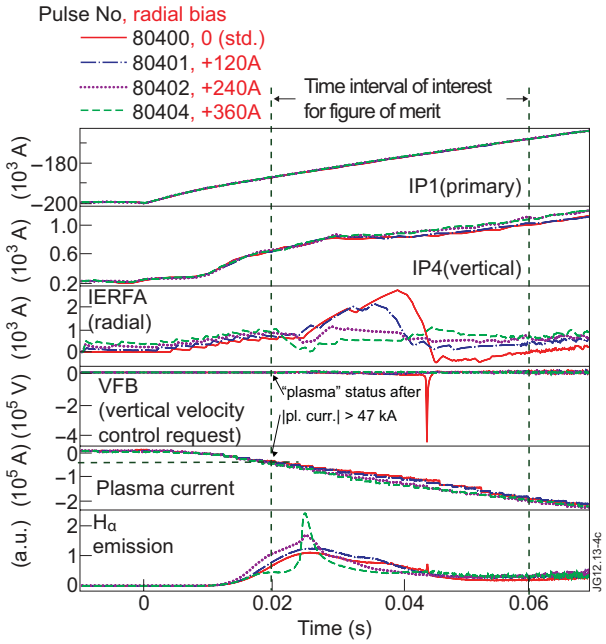

Figure 4: Experimental results for the breakdown optimization activity. In the different plots are reported the data regarding four different JET pulses where a progressive radial bias correction was added, starting from the standard one (radial bias = 0). In the first two plots are shown the primary and vertical circuits currents. In the third plot is shown the radial field circuit current. In the fifth plots is reported the plasma current value, while in the last plot is reported one of the H-Alpha emission lines, used to reveal the plasma start.

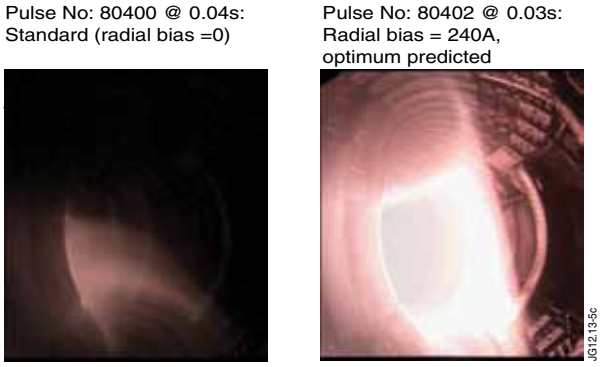

Figure 5: Comparison of the two first available images from the slow JET visible camera (25 frames/sec). By applying an optimised correction radial bias the plasma starts further from the divertor region, as from the model prediction, comparing with the standard case.

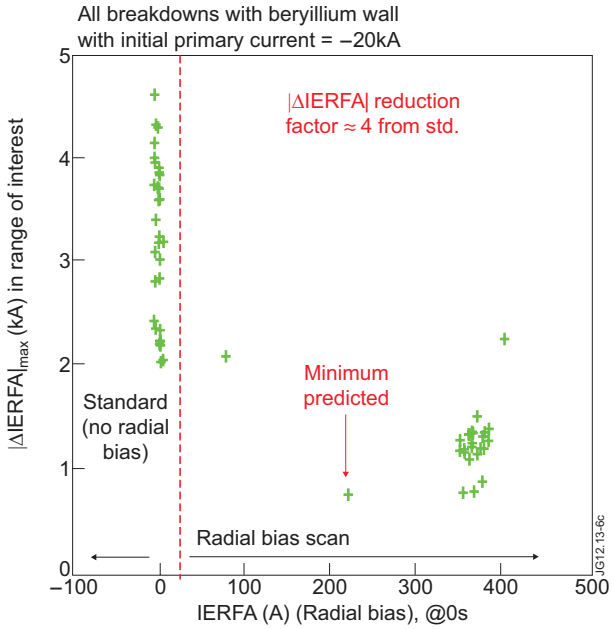

Figure 46: In the plot is reported a statistical analysis for all the breakdowns obtained at JET after the installation of the beryllium wall, for the configuration with primary current equal to 20 kA. On the abscissa axis is shown the value of the ERFA current at the breakdown start, which is proportional to the requested correction radial field. The vertical dashed line distinguishes the standard non optimised pulses, with no radial bias, to the left, and the radial bias scan to the right. In the ordinate axis is reported the figure of merit considered.

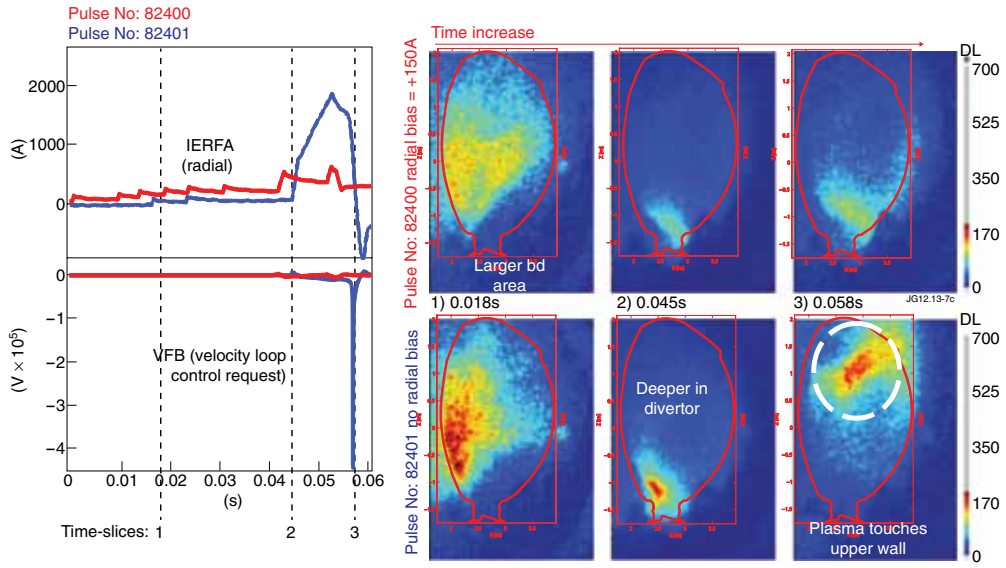

Figure 7: Comparison of experimental data and recorded images from the fast visible camera, for a standard and an optimised breakdown. In the plots on the left are reported the radial field current excursion and velocity loop request for the two cases. The vertical dashed lines indicate the time slices in correspondence of the three couple of images for the two pulses.

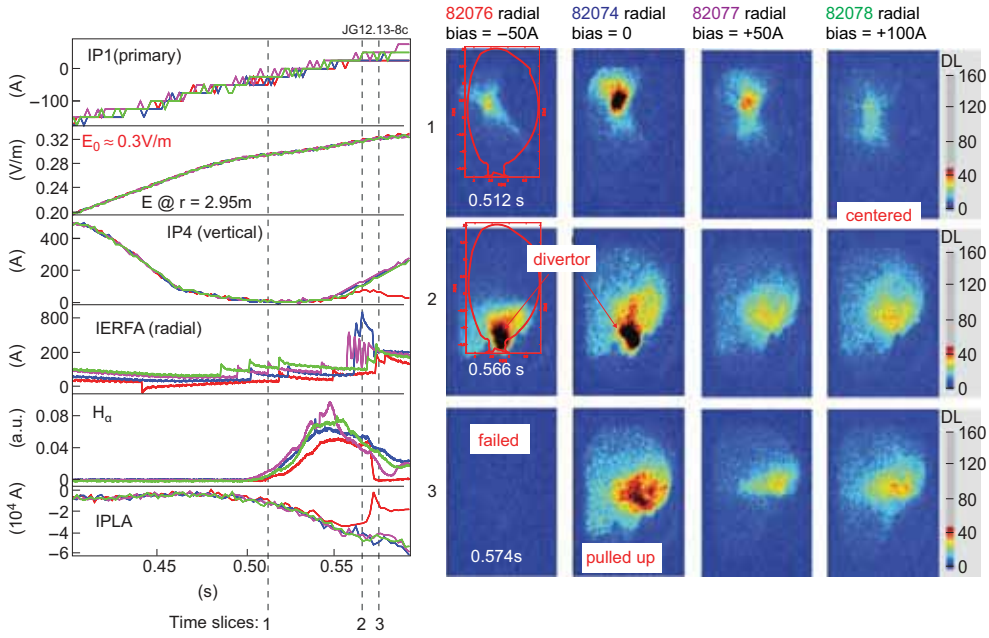

Figure 8: Experimental data and images from the JET fast visible camera for a radial bias scan with initial primary current IP1 around zero. The vertical dashed lines in the experimental plots indicate the time where the pictures are captured. In the plots on the left are shown the primary current, the electric field at r = 2.95 m, the vertical and radial field currents. In the last two plots are shown one of the H-Alpha emission lines, and the plasma current evolutions.